Biomatter 4, e28823; April 2014; © 2014 Landes Bioscience

Nanotemplated polyelectrolyte films as porous biomolecular delivery systems

Application to the growth factor BMP-2

Adeline Gand[1], Mathilde Hindié[1], Diane Chacon[1], Paul R Van Tassel[2], and Emmanuel Pauthe[1,*]

[1]Equipe de Recherche sur les Relations Matrice Extracellulaire Cellules; Institut des Matériaux; Université de Cergy-Pontoise; Cergy-Pontoise, France;
[2]Department of Chemical and Environmental Engineering; Yale University; New Haven, CT USA

Keywords: delivery system, BMP-2, polyelectrolyte, layer-by-layer, porous material, biomaterial, cell differentiation

Biomaterials capable of delivering controlled quantities of bioactive agents, while maintaining mechanical integrity, are needed for a variety of cell contacting applications. We describe here a nanotemplating strategy toward porous, polyelectrolyte-based thin films capable of controlled biomolecular loading and release. Films are formed via the layer-by-layer assembly of charged polymers and nanoparticles (NP), then chemically cross-linked to increase mechanical rigidity and stability, and finally exposed to tetrahydrofuran to dissolve the NP and create an intra-film porous network. We report here on the loading and release of the growth factor bone morphogenetic protein 2 (BMP-2), and the influence of BMP-2 loaded films on contacting murine C2C12 myoblasts. We observe nanotemplating to enable stable BMP-2 loading throughout the thickness of the film, and find the nanotemplated film to exhibit comparable cell adhesion, and enhanced cell differentiation, compared with a non-porous cross-linked film (where BMP-2 loading is mainly confined to the film surface).

Introduction

Controlling the cellular response represents a key challenge in biomaterials science/engineering. Materials capable of presenting or releasing bioactive species (e.g., proteins, peptides, nucleic acids)—chosen so as to elicit (a) specific biological response(s)—represent a promising avenue. Biomolecular delivery systems of controlled spatial and temporal release are of particular interest for a broad variety of biomedical applications, such as drug delivery, tissue engineering, biosensing and regenerative medicine.

Thin films formed via the Layer-by-Layer (LbL) assembly of oppositely charged macromolecules[1] are excellent candidates for biomaterial applications involving cell-material contact.[2-5] LbL films are easy to fabricate, can be used to modify the surface of many types of materials, irrespective of shape, and possess physicochemical properties that are readily controllable. Moreover, LbL films can be rendered bioactive via surface adsorption or direct incorporation of biomolecules.

The ability of an LbL film to serve as a biomolecular reservoir/delivery system has been investigated using polymers that degrade based on (1) enzymes released by the cell[6,7] and (2) hydrolysis.[8-13] These studies have successfully demonstrated LbL film bioactivity, based on a governing mechanism whereby bioactive species become accessible to cells via film degradation.

In addition to the presence of bioactive elements, cells respond to the mechanical nature of the contacting material. In their native (as-built) state, LbL films are generally too soft to promote robust cell adhesion, so many studies have explored enhancing film rigidity via chemical cross-linking of the polymer network.[14-19] While successful at improving mechanical properties, chemical cross-linking is known to suppress film degradation, and thus would be incompatible with the biomolecular delivery strategies summarized above. In addition, the cross-linking chemistry itself could compromise bioactivity by directly affecting the function of the bioactive species.

Previously, we developed a porous film strategy toward the independent control of LbL film mechanical rigidity and biomolecular delivery.[20] The approach involved introducing charged latex nanoparticles (NP) during film formation, followed by chemical cross-linking of the polymer network. The NP were dissolved by organic solvent exposure, leading to pore formation within the film. The idea is to control film bioactivity through the extent of pore loading, and film mechanical properties by the extent of cross-linking. These films were shown to possess enhanced mechanical rigidity and high bioactive species loading.

In this paper, we investigate the use of porous LbL films to efficiently deliver an osteoconductive growth factor, the recombinant human bone morphogenic protein-2 (BMP-2), and to

*Correspondence to: Emmanuel Pauthe; Email: emmanuel.pauthe@u-cergy.fr
Submitted: 01/09/2014; Revised: 03/21/2014; Accepted: 04/08/2014; Published Online: 04/17/2014
Citation: Gand A, Hindié M, Chacon D, van Tassel PR, Pauthe E. Nanotemplated polyelectrolyte films as porous biomolecular delivery systems: Application to the growth factor BMP-2. Biomatter 2014; 4:e28823; PMID: 24743114; http://dx.doi.org/10.4161/biom.28823

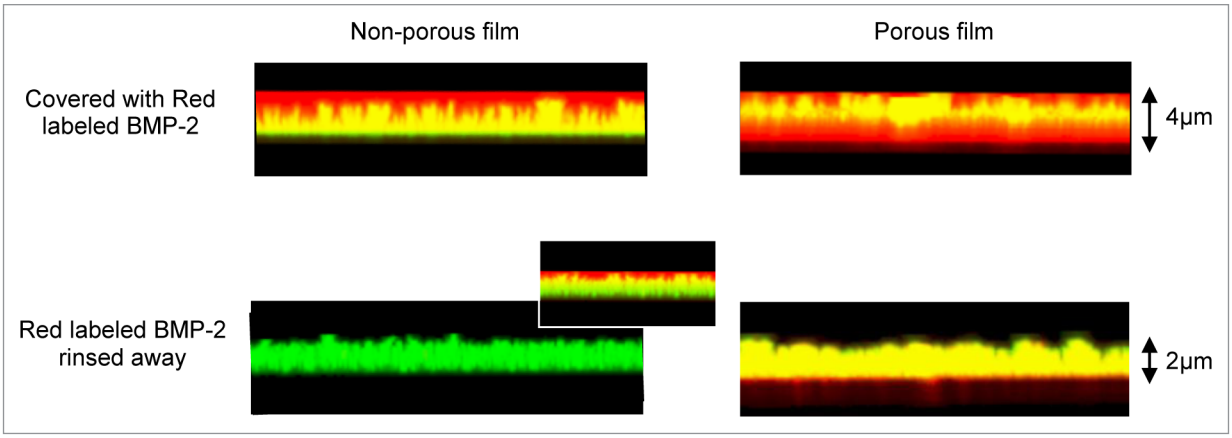

Figure 1. Laser scanning confocal microscopy images of cross-linked $(PLL\text{-}PGA)_{26}$ films (non-porous film) and of cross-linked $([PLL\text{-}PGA]_5\text{-}PLL\text{-}NP)_4\text{-}(PLL\text{-}PGA)_2$ films treated with THF to remove the NP (porous film). In both case, the penultimate PLL is labeled with FITC (green) and diffuses freely within the film[25] so that the entire film appears green. Upper part: cross-sectional micrographs of films covered with red labeled BMP-2. Lower part: cross-sectional micrographs of films after three rinsing steps with buffer. Laser intensities are 1% and 0.1%, respectively, for excitation wavelength 488 nm and 561 nm. The inset shows the non-porous film rinsed with laser intensities of 1% for both the 488 nm and the 561 nm lasers, and shows some red labeled BMP-2 to remain at the surface of the film.

direct the differentiation of myoblastic C2C12 cells into osteoblasts. BMP-2 is used clinically for its osteoinductive properties toward bone formation and reconstruction, and has shown promising results in spinal fusion, fracture repair and oral/maxillofacial reconstruction.[21] The doses applied in clinical treatment are typically high and non-physiological, and could lead to important complications such as bone tissue overgrowth, inflammation or cancer.[22,23] Many applications would be better served by the local delivery, at lower concentration, of BMP-2; we seek here to address this need via porous, polyelectrolyte-based thin films.

Results

Films characterization

We consider LbL films composed of poly(L-lysine) (PLL) as polycation, and poly(L-glutamic acid) (PGA) and carboxyl functionalized latex nanoparticles (NP) as polyanions. Three different systems are considered: (1) native films consisting of $(PLL\text{-}PGA)_n$ (n standing for the number of bilayers), (2) cross-linked (non-porous) films consisting of $(PLL\text{-}PGA)_n$ and subsequently exposed to EDC-NHS chemical cross-linking agents, and (3) templated, cross-linked (porous) films consisting of $([PLL\text{-}PGA]_2\text{-}PLL\text{-}NP)_n\text{-}(PLL\text{-}PGA)_2$, subsequently exposed to EDC-NHS chemical cross-linking agents, and finally exposed to tetrahydrofuran to dissolve the NP.

The mechanical rigidity of cross-linked $(PLL\text{-}PGA)_{26}$ films (non-porous), and cross-linked $([PLL\text{-}PGA]_5\text{-}PLL\text{-}NP)_4\text{-}(PLL\text{-}PGA)_2$ films exposed to THF (porous) is determined via nano-indentation analysis in which a probe of known tip geometry is pressed into the material surface, and the resultant force measured. Mechanical hardness is expressed as $H = \frac{F_{max}}{A(h_c)}$, where F_{max} is the maximum force during a nano-indentation experiment, $A(h)$ is the cross-sectional area of the indentation probe as a function of axial distance from its tip (h), and h_c is the axial distance from the probe's tip over which material/probe contact occurs during the maximum applied force.[24] Based on a maximum load of 40 N (corresponding to indentation magnitudes of about 150 nm, or about 2% of the overall film thickness), and using established methods to estimate h_c from force vs. indentation curves,[24] we find the hardness of the non-templated, cross-linked film to be 220 ± 20 kPa, and that of the templated cross-linked film to be 190 ± 20 kPa. We conclude templated, chemically cross-linked films to be of comparable mechanical rigidity to non-templated, chemically cross-linked films.

Nanoparticle dissolution and pore space formation are demonstrated using direct and indirect analysis. Prior work shows THF treatment of native films (i.e., without crosslinking) containing latex nanoparticles to result in significant film collapse, suggesting removal of the nanoparticles from the film.[20] In contrast, cross-linked films did not exhibit such a collapse, suggesting in this case the particle removal to be accompanied by formation of pore space.[20] UV spectra of THF used to dissolve the nanoparticles from the film exhibit peaks that are also found in a latex sample, suggesting the presence of latex in the dissolving solution and hence nanoparticle removal from the film (see **Supplemental Materials**).

Prior AFM analysis showed all films to be topographically quite smooth, with the root mean square roughness of the templated film (10 nm) approximately intermediate between that of the native (7 nm) and the NP containing native (13 nm) film.[20]

Film loading of BMP-2

We assess the loading of porous and non-porous films to BMP-2 by laser scanning confocal microscopy. The film is fluorescently labeled green using PLL dyed with FITC, and BMP-2 is labeled red with Alexa Fluor 568. In **Figure 1**, we show

a cross-sectional micrograph of a non-porous cross-linked $(PLL\text{-}PGA)_{26}$ film, and a porous cross-linked $([PLL\text{-}PGA]_5\text{-}PLL\text{-}NP)_4\text{-}(PLL\text{-}PGA)_2$ film, each treated with THF. (Films subjected to confocal analysis contain more layers than do films used in other experiments, as thicker films allow for enhanced optical resolution of fluorescent species.) The penultimate layer of these films contains a fluorescently labeled polycation (PLL-FITC). PLL-FITC (as well as unlabeled PLL) has been previously shown to freely diffuse throughout the film,[25] and so the entire film appears green.[20] When subjected to red labeled BMP-2, both films appear mainly yellow, and the solution above red. Nevertheless, we clearly observe that for the non-porous film, a thin band of green is still visible at the bottom of the film, whereas for the porous film, the bottom of the film appears red, suggesting a greater degree of film penetration in the case of the porous film. After extensive rinsing, the non-porous film appears completely green, whereas the porous film remains mainly yellow. A large part of the BMP-2 is still present on and within the porous film. It is necessary to overexpose—by increasing the laser intensity of the 561 nm excitation wavelength (Alexa Fluor 568) to 1%—the non-porous film treated with red-labeled BMP-2 to observe some red color at the film surface, suggesting the presence of residual adsorbed BMP-2.

These results show enhanced film permeability to BMP-2 of the porous vs. the non-porous film, and a post-rinse BMP-2 distribution covering the entire film only in the case of the porous film, where BMP-2 enters, diffuses through the film, and remains trapped. This observation is in agreement with previous studies that showed BMP-2 labeled with Rhodamine to accumulate in the upper part of a chemically cross-linked (non-templated) LbL film.[26]

We also assess film loading of BMP-2 by quartz crystal microgravimetry with dissipation analysis (QCM-D, **Fig. 2**). A non-porous cross-linked $(PLL\text{-}PGA)_{14}$ film, and a porous cross-linked $([PLL\text{-}PGA]_5\text{-}PLL\text{-}NP)_2\text{-}(PLL\text{-}PGA)_2$ film are assembled on quartz sensors and subjected to 15 min contact with 150 ng of BMP-2, followed by 5 buffer rinsing steps of 2 min. We observe the difference in resonator frequency change to be around 5 times higher for the porous vs. the non-porous film. Moreover the change in signal during the rinse steps is 85% for the non-porous film and 15% for the porous film. These results suggest BMP-2 association with a non-porous film to be highly reversible and result (after rinsing) in a low/weak BMP-2 adsorption at the surface, and BMP-2 association with porous film to result in stable loading throughout the film volume, consistent with our confocal microscopy results.

Film release of BMP-2

In **Figure 3**, we show cross-sectional micrographs of green labeled films incubated with red labeled BMP-2, following 2 h and 72 h of buffer exposure. At both time points, the non-porous film appears green, suggesting most BMP-2 previously adsorbed at the surface to be released / desorbed.

We observe the porous film to be yellow at 2 h, suggesting a significant quantity of BMP-2 to be retained and to be distributed fairly uniformly within the film. At 72 h, we observe the yellow intensity to decrease, the top of the film to appear green, and the bottom of the film to exhibit some red spots. This result suggests a release of BMP-2 between 2 h and 72 h, occurring preferentially from the top of the film. Moreover, after 72 h, a significant quantity of BMP-2 appears to be retained in the film, with an apparent inhomogeneous distribution of higher concentration at the base of the film.

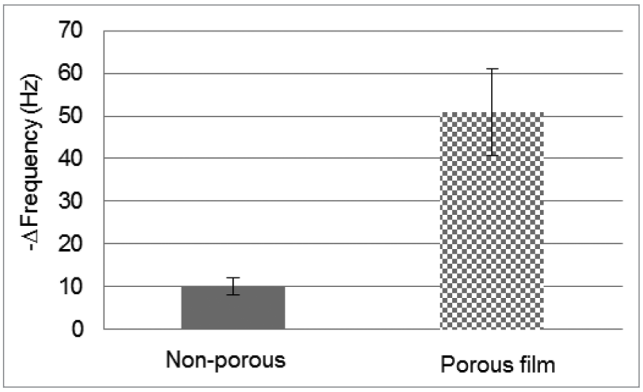

Figure 2. Quartz crystal microgravimetry measurements of BMP-2 loading onto/within cross-linked $(PLL\text{-}PGA)_{14}$ (non-porous) and cross-linked $([PLL\text{-}PGA]_5\text{-}PLL\text{-}NP)_2\text{-}(PLL\text{-}PGA)_2$ exposed to THF (porous) films. Both films are incubated with 150 ng of BMP-2 (during 15 min) then extensively rinsed with buffer (10 min total).

C2C12 proliferation and morphology

We next consider the proliferation and morphology of murine C2C12 myoblasts, whose adhesion and organization has been previously shown to be enhanced on LbL films of increased mechanical rigidity.[27] Cells are cultured on three types of films: non-cross-linked $(PLL\text{-}PGA)_{14}$ (native, negative control), cross-linked $(PLL\text{-}PGA)_{14}$ (non-porous, positive control), and cross-linked $([PLL\text{-}PGA]_5\text{-}PLL\text{-}NP)_2\text{-}(PLL\text{-}PGA)_2$ exposed to THF (porous). Proliferation and morphology are observed following 48 h culture. In **Figure 4A**, we show C2C12 proliferation to be enhanced, to similar extents, on non-porous and porous films (compared with native films). Moreover, no differences in cell adhesion and early spreading are observed between non-porous and porous films (data not shown). When cultured on non-porous and porous films for 48 h, cells spread with long pseudopodia and focal contacts, whereas on native films, the cells are round shaped with no clear vinculin plaques or stress fibers (**Fig. 4B**). Moreover, C2C12 cells cultured on porous films present more focal adhesions organized in lamellipodia than do those cultured on cross-linked films. Overall, cells are observed to develop more and better organize adhesion structures when cultured on porous films.

Altogether, these results suggest porous films to promote C2C12 cell attachment, spreading, organization, and proliferation at a level similar to that of (positive control) non-porous film, and at a level significantly higher than that of (negative control) native films. We observe no direct effect of pore formation and THF treatment on cell behavior, consistent with previous observations on pre-osteoblastic MC3T3-E1 cells.[20]

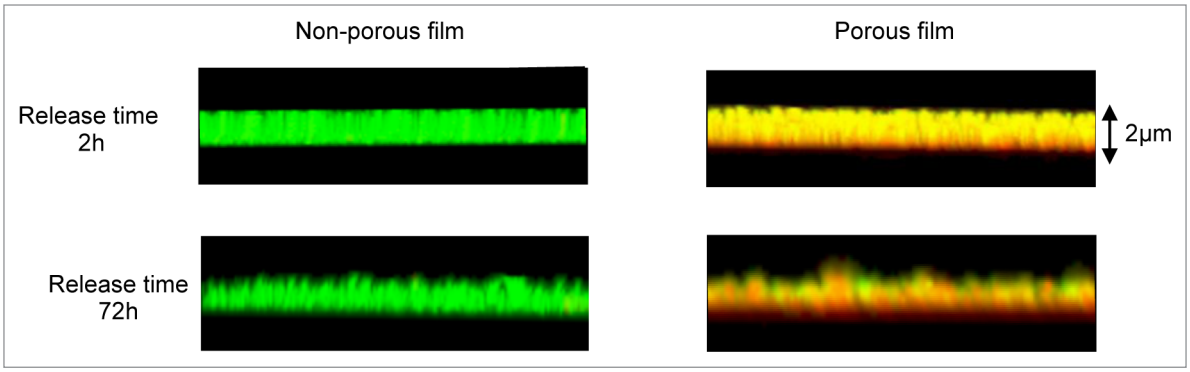

Figure 3. Laser scanning confocal microscopy images of BMP-2 desorption from cross-linked $(PLL\text{-}PGA)_{26}$ films (non-porous) and from cross-linked $([PLL\text{-}PGA]_5\text{-}PLL\text{-}NP)_4\text{-}(PLL\text{-}PGA)_2$ films treated with THF to remove the NP (porous film). BMP-2 desorption is followed after 2 h and 72 h incubation in PBS buffer pH 7.4. In both cases, the non-porous film appears green, suggesting little BMP-2 to remain onto/within the film. On the contrary, after 72 h, some red spots are still visible in the porous film, suggesting an appreciable fraction of BMP-2 to remain in the film.

Film bioactivity

The bioactivity of BMP-2 loaded onto/within non-porous *vs* porous thin films may be assessed using murine C2C12 myoblasts modified with a luciferase gene fused to a BMP-responsive element (BRE).[28] Films are exposed to 10, 50 or 500 ng of BMP-2 in 1mM HCl for 16h. Following a buffer rinse, cells are seeded and cultured for 24 h. In **Figure 5**, we show luciferase activity to increase proportionally to the quantity of BMP-2 exposed to the film. Similar luciferase activity is observed between non-porous and porous films with 10 ng of BMP-2, but significantly higher activity is observed for porous films with 50 and 500 ng. This result suggests porous films to be more efficient than non-porous films in terms of presenting active BMP-2 to contacting cells.

BMP-2 bioactivity is also investigated in terms of a shift in the differentiation pathway from myoblastic to osteoblastic. When cultured in a medium containing a low concentration of serum, and especially in absence of growth factor (i.e., BMP-2), C2C12 cells differentiate into contractile myoblasts. However, treatment with BMP-2 cause a shift in the differentiation pathway from myoblastic to osteoblastic.[29,30]

C2C12 cells are seeded on non-porous or porous films previously loaded or not with 500 ng of BMP-2 in a low serum containing medium. After 7 d of culture, the cells are fixed and immunostained for myosin heavy chain (late marker of myogenic differentiation) and osteopontin (early marker of osteoblastic differentiation). In **Figure 6**, we show that in the absence of BMP-2, the myosin expression is high. The presence of myocytes, characteristic of cell differentiation into myotubes, is evident. When the films are loaded with 500 ng of BMP-2 we observe, on a non-porous film, the myosin expression to be slightly decreased and a lower osteopontin expression to be visible. In the case of a porous film, no myosin expression is observed, and a large osteopontin expression is evident. Clearly, the markers of osteoblastic differentiation are expressed to a significantly greater extent in cells cultured on the porous compared with the non-porous film.

This result suggests, in the absence of BMP-2, the cells to differentiate to myocytes and myotubes (on both films), and in the presence of BMP-2, the cells to differentiate into osteocytes. The differentiation into osteocytes is more pronounced on porous compared with non-porous films, suggesting an enhanced exposure to bioactive BMP-2 in the porous film. Interestingly, the quantity of BMP-2 present in the porous film after 7 d is sufficient to induce cell differentiation to osteocytes.

Discussion

Thin polyelectrolyte films are of particular interest as they could have a broad impact in numerous cell-contacting applications. One can envision thin film coatings for biomedical devices (e.g., stents), cell-based bioreactor supports and tissue engineering scaffolds. They also show significant potential to locally and temporally deliver bioactive molecules from the coating of an implantable device.

Cells respond to bioactive species adsorbed at the surface or embedded within the film, as well as to the physicochemical properties of the film itself. Previous studies have shown as-built polyelectrolyte-based thin films to be highly hydrated and very soft, and thus to be unfavorable for primary cell adhesion.[31] Chemical cross-linking can increase film stiffness, and has been shown to greatly enhance the adhesion, spreading and proliferation of certain cell types.[16,18,32,33] However, chemical cross-linking generally compromises bioactivity, as described below.

Thin polyelectrolyte films may be rendered bioactive by the loading/incorporation of bioactive molecules such as drugs, peptides, proteins or DNA. The bioactive molecules can be integrated within the films using different strategies. In one approach, biomolecules can be embedded within the film by direct integration during film assembly, and accessed by contacting cells via cell-induced film degradation,[6,7] or released subsequently by hydrolytic film degradation.[9,10,34-37] In this case, post-assembly cross-linking could compromise film bioactivity due to a loss of biomolecular mobility within the film,[6,7,19] and suppression of film degradation.[38-41] As an alternative strategy, biomolecules can be loaded in the films after assembly and cross-linking via a simple diffusion mechanism. Polyelectrolyte-based thin films formed by LbL assembly have been shown to serve as reservoirs for small molecules such as the anti-cancer

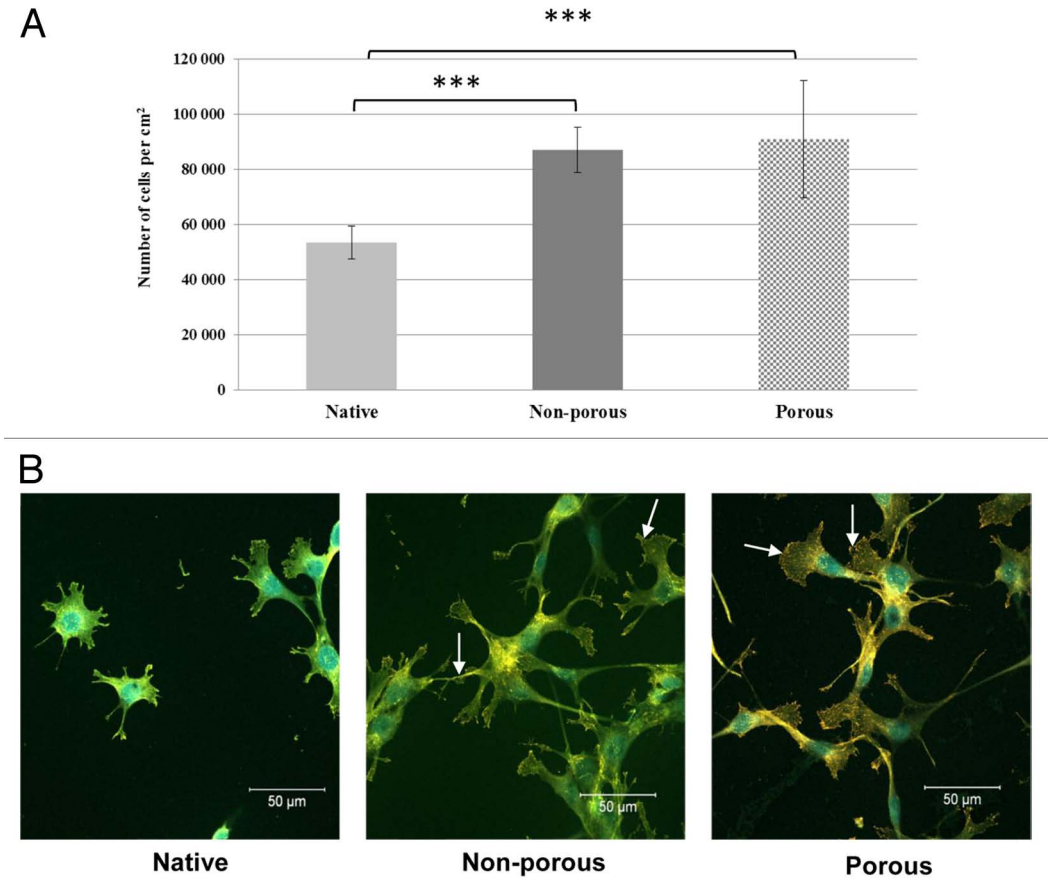

Figure 4. Cell proliferation (**A**) and morphology (**B**) on $(PLL\text{-}PGA)_{14}$ (native), cross-linked $(PLL\text{-}PGA)_{14}$ (non-porous), and cross-linked $([PLL\text{-}PGA]_5\text{-}PLL\text{-}NP)_2\text{-}(PLL\text{-}PGA)_2$ exposed to THF (porous). The cells are cultured for 48 h in complete medium, counted after being detached from the substrates (**A**) or stained (**B**): actin (green), nuclei (blue) and vinculin (red). Arrows indicate focal adhesions.

drug paclitaxel and the anti-inflammatory drug diclofenac.[39,42] These small molecules were shown to diffuse through the entire film thickness, even in the case of a cross-linked film. However, the permeability of cross-linked films to molecules of higher molecular weight, such as protein or peptides, is more limited. For example, the adsorption of BMP-2 growth factor (27 kDa) mainly occurs at the surface of the films.[26,43-45] A potential means to increase film permeability to high molecular weight molecules is to create porosity within the films.

We previously developed a cross-linked, nanoparticle templated film where the porosity is introduced after the dissolution of carboxyl latex nanoparticles introduced during film assembly.[20] We showed these films to be sufficiently rigid so as to promote initial cell adhesion, spreading and viability, and to be capable of significant biomolecular species loading. Since film rigidity may be controlled through the extent of cross-linking, and film bioactivity through the degree of pore loading, this approach potentially allows for the independent control of film mechanical rigidity and bioactivity.

In this paper, we show templated film mechanical rigidity to be sufficient to enhance adhesion, spreading and proliferation of myoblastic C2C12 cells, compared with a softer, native film. Moreover, the growth factor BMP-2 can be loaded throughout the thickness of the film, with a post-rinse loading that is 5-fold greater than that of a non-porous film (where loading occurs preferentially to the film surface). A large fraction is retained following 72 h, compared with the native film where release is rapid and nearly complete. Most significantly, C2C12 cells respond to BMP-2 functionalized porous films to a significantly greater extent than they do to BMP-2 functionalized non-porous films, suggesting the BMP-2 to be loaded and released in a bioactive form.

Certain details remain unknown concerning the distribution and release of BMP-2 within porous and non-porous films. Although our confocal micrographs suggest a certain degree of BMP-2 penetration within non-porous films, the fact that most of the growth factor is rapidly removed upon simple buffer rinsing suggests that the initial loading may have occurred primarily at the film surface. Indeed, the fraction released within the porous system, which would be expected to be more reversible owing to adsorption within much larger pores, is significantly less that that within the non-porous system. Future work toward quantifying the loading distribution and release kinetics would greatly clarify this picture, and is needed to ultimately engineer growth factor loaded polyelectrolyte based films for biomedical applications.

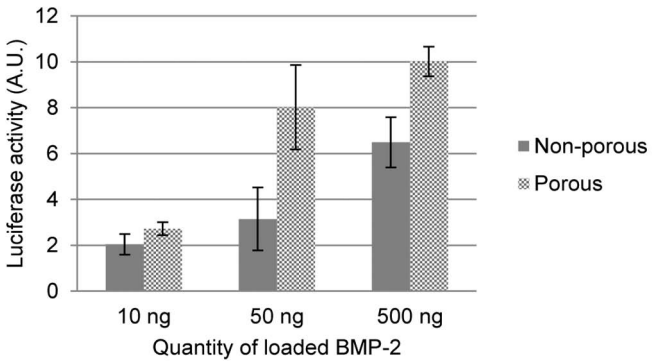

Figure 5. Bioactivity induced by BMP-2 loaded onto/within non-porous and porous thin films. BMP-2 bioactivity is determined by measuring the luciferase expression of C2C12-BRE/Luc cells. The cells are cultured for 24 h on cross-linked $(PLL\text{-}PGA)_{14}$ (non-porous) and cross-linked $[(PLL\text{-}PGA)_5\text{-}PLL\text{-}NP]_2\text{-}(PLL\text{-}PGA)_2$ exposed to THF (porous) films loaded with 10, 50 or 500 ng/L of BMP-2. The results are normalized with the controls made in absence of BMP-2.

Open questions also persist concerning the role of any residual latex in the film, following template removal. While prior analysis of (non-cross-linked) film collapse upon organic solvent (THF) exposure,[20] and current UV spectroscopic evidence of latex in THF exposed to the template film, together suggest significant latex removal, the possibility remains that some latex is left behind. This residual latex could serve to bind to the growth factor and contribute to its slow release kinetics. In any event, we observe no adverse effects of any residual latex on the contacting cells or on the bioactivity of the embedded BMP-2. Future work toward quantifying any residual latex may help to clarify this picture.

The C2C12 cell system was chosen owing to its known surface adhesion dependence on substrate rigidity, and the experimental ease of measuring the cellular response to BMP-2. In addition, it represents a highly relevant progenitor cell system for bone tissue engineering.

Previous studies have also employed LbL films as delivery systems for BMP-2. Hammond et al., showed the incorporation of BMP-2 into a soft, hydrolytically degradable film built on top of a non-degradable cross-linked film to permit the delivery of the growth factor over 7 d, and to promote the differentiation of mesenchymal stem cells to osteoblasts.[35] Picart, et al. adsorbed BMP-2 to the surface of cross-linked films in an amount that was sufficient to induce C2C12 myoblastic cell differentiation into osteoblasts.[26] In comparison to these previously reported systems, our templated films offer some potential advantages. Compared with hydrolytically degradable films, templated films may be rigidified to favor cell adhesion, without compromise of bioactivity. Compared with surface adsorption, embedding biomolecules within porous films allows for higher loading and temporally controlled delivery, and keeps the surface free for other species aimed at favoring initial cell adhesion and/or preventing adsorption of non-desirable biomolecular species or bacterial infection.

Porous films loaded with BMP-2 could be ideal coatings for bone tissue engineering scaffolds and/or bone implant devices. In both cases, film rigidity may be optimized to promote initial cell adhesion, and BMP-2 loading and release may be optimized to promote timely differentiation of progenitor cells toward an osteoblastic lineage, potentially favoring a strong bone-material interface. Orthopedic implants often fail due to poor integration with bone tissue, as occurs when a fibrous tissue capsule forms around the implant in preference to bone; porous polyelectrolyte films would appear to be an excellent strategy toward a mechanically robust bone-implant interface.

Conclusion

We demonstrate here nanoparticle templating as a means toward porous LbL films of controlled biomolecular loading and release. We show the mechanical rigidity of—and the myoblastic C2C12 cell adhesion, spreading and proliferation on—templated films to equal those on (positive control) non-templated films. Templated films additionally exhibit significant growth factor (BMP-2) loading and retention over 72 h, and are shown to induce C212 differentiation into osteoblasts.

Materials and Methods

Film Assembly

Films are assembled on 10 mm diameter glass slides, squared glass microscope slides or QCM-D sensor chips previously washed with detergent and rinsed with deionized water. $(PLL\text{-}PGA)_n$ and $([PLL\text{-}PGA]_5\text{-}PLL\text{-}NP)_n\text{-}(PLL\text{-}PGA)_2$ films are assembled by subsequent dipping in 0.1 g/L Poly-L-Lysine (PLL, MW 70–150 kDa, Sigma) and Poly-L-Glutamic acid (PGA, MW 50–150 kDa, Sigma) in PBS pH 7.4, and 1 g/L carboxyl functionalized latex nanoparticles (C37261, Invitrogen), of diameter 28 ± 4 nm diluted in deionized water when necessary. Each dipping step last for 10 min followed by three 1 min buffer rinse steps. Both films are subjected to chemical cross-linking with 40 mM 1-ethyl-3-(3 [dimethylamino]propyl)carbodiimide (EDC, Sigma) and 100 mM, *N*-hydroxysulfosuccinimide (sulfo-NHS, Sigma) for 16h. The films containing the carboxyl functionalized latex nanoparticles (NP, Invitrogen) are incubated in tetrahydrofurane (THF) for 16h in order to remove the NP from the films and rinsed three times for 20 min in buffer, as previously described.[20] Native $(PLL\text{-}PGA)_n$ films are formed as described above, but without chemical EDC-NHS cross-linking.

Nanoindentation

Nanoindentation involves a probe of known geometry and mechanical properties being pressed into a material sample, with precise measurement of force and displacement. A CPX-UNHT Ultra Nanoindentation Tester (CSM Instruments) is employed with a ruby spherical indenter of 200 mm radius, loading and unloading rates of 60 mN/min, and a maximum load of 40 mN, on polyelectrolyte films formed on glass microscope slides.

BMP-2 labeling

BMP-2 (Millipore) was resuspended in HCl 1 mM and stored at -20 °C until use. For BMP-2 fluorescent labeling, 1 µg of BMP-2 is diluted in 1 mL carbonate-bicarbonate buffer in order to raise pH 8.3. Five µL of Alexa Fluor 568 (AF-568 10mg/mL, Invitrogen) is added to the BMP-2 solution and incubated for 16 h at room temperature. The mixture is then subjected to dialysis against PBS pH 7.4 in order to remove the unbounded dye. The molar grafting ratio was estimated by the BMP-2 and AF-568 concentrations, and is determined to be about 1.4.

Confocal microscopy

The permeability to BMP-2 of cross-linked $(PLL\text{-}PGA)_{26}$ films (non-porous) and cross-linked $([PLL\text{-}PGA]_5\text{-}PLL\text{-}NP)_4\text{-}(PLL\text{-}PGA)_2$ films treated with THF (porous film) is assessed using a LSM710 confocal microscope (Carl Zeiss). In this case, the penultimate PLL layer is labeled with FITC (Invitrogen) and freely diffuses through the films.[25] The images are recorded using laser intensities of 1% for the laser 488 nm and 0.1% or 1% for the laser 561 nm.

The release of AF-568 BMP-2 from the films is determined after 2 h and 72 h exposure to PBS pH 7.4. Images are recorded using laser intensities of 1% and 0.5%, respectively at wavelengths 488 nm and 561 nm.

BMP-2 loading

Films are exposed to 100 µL of 0.1 g/L AF-568 labeled BMP-2 (AF-568 BMP-2) for 1 h at room temperature, and then rinsed three times for 1 min in PBS pH 7.4.

Quartz Crystal Microgravimetry with Dissipation (QCM-D)

Experiments were performed using a D300 system (Q-Sense, Sweden) using a QAFC302 flow chamber and QSX303 Sensor Chip (Q-sense) consisting of a planar SiO_2 coating on a quartz crystal. This technique consists of measuring changes in frequency and dissipation factor of the quartz crystal sensor. The resonant frequency of the crystal depends on the total oscillating mass, including coupled water.[46]

The sensor chips covered with cross-linked $(PLL\text{-}PGA)_{14}$ films (non-porous) and cross-linked $([PLL\text{-}PGA]_5\text{-}PLL\text{-}NP)_2\text{-}(PLL\text{-}PGA)_2$ films treated with THF (porous) are inserted into the flow cell. A PBS pH 7.4 solution is introduced until a steady baseline is achieved and 150 ng of BMP-2 in PBS pH 7.4 is introduced for 15 min, followed by a 10 min buffer rinse.

Cell culture

C2C12 cells are maintained in polystyrene flasks in an incubator at 37 °C and 5% CO_2, and cultured in Dulbecco's modified Eagle's medium high glucose (DMEM high glucose)/ Glutamax (Invitrogen) supplemented with 10% fetal bovine serum (PAA laboratories), 100 U/mL penicillin G and 100 µg/mL streptomycin (Eurobio) (Complete medium). Cells are subcultured before reaching confluence (60–70% confluence).

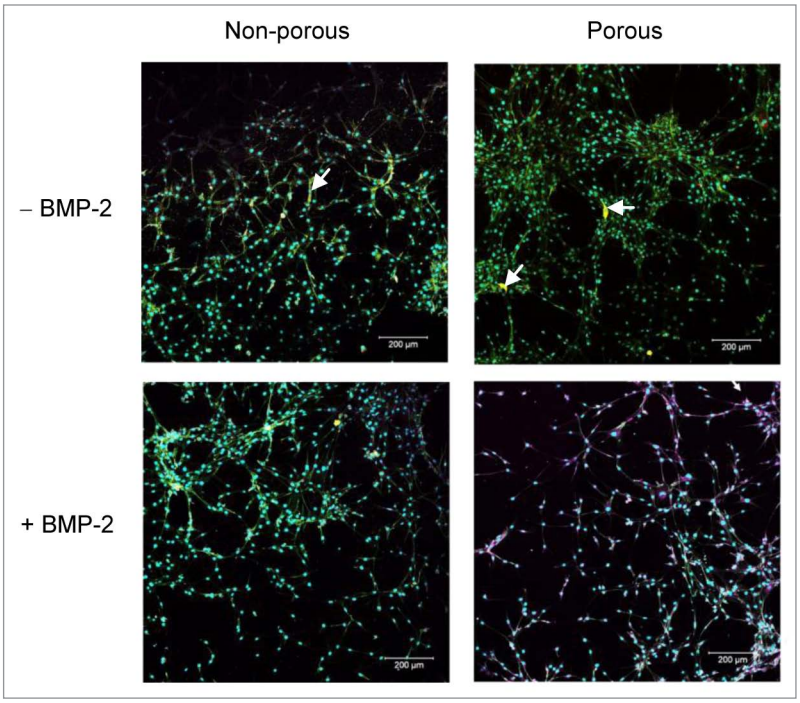

Figure 6. Influence of BMP-2 loaded in non-porous and porous films on cell differentiation. C2C12 cells are cultured for 7 d on cross-linked $(PLL\text{-}PGA)_{14}$ (non-porous) and cross-linked $([PLL\text{-}PGA]_5\text{-}PLL\text{-}NP)_2\text{-}(PLL\text{-}PGA)_2$ exposed to THF (porous) films in absence of BMP-2 (top panels) or loaded with 500 ng BMP-2 (lower panels). Heavy chains of myosin are shown in yellow and osteopontin in magenta. Arrows indicate myocytes. BMP-2 is seen to promote an osteoblastic differentiation that is more pronounced in the porous film system.

C2C12 BRE/Luc cells are C2C12 cells stably transfected with a bone-responsive element fused to the luciferase gene.[28] They are maintained in complete medium added with Geneticin (G418, Invitrogen) 200 µg/mL.

Cell proliferation and morphology

To measure cell proliferation, 10000 C2C12 cells/cm^2 are seeded on 10 mm glass slides covered with cross-linked $(PLL\text{-}PGA)_{14}$ films (non-porous) and cross-linked $([PLL\text{-}PGA]_5\text{-}PLL\text{-}NP)_2\text{-}(PLL\text{-}PGA)_2$ films treated with THF (porous), and cultured in complete medium. After 24 and 48 h of culture, cells are detached from substrates by trypsinization and counted in a Malassez hemocytometer. All experiments are performed in triplicate.

Cell morphology is observed after 48 h of culture. Cells are fixed with 3% (w/v) para-formaldehyde solution dissolved in PBS (Sigma) for 15 min, then permeabilized with 1% (v/v) Triton X-100 (Sigma) for 15 min. Non-specific binding sites are blocked by incubating the substrates in PBS containing 1% Bovine Serum Albumine (BSA) for 30 min. Substrates are then incubated, for 1 h, with 100 µg/ml mouse polyclonal anti-vinculin antibodies (Sigma) dissolved in PBS containing 0.1% BSA. Bound specific antibodies are revealed by incubation with 100 µg/ml TRITC coupled secondary antibodies (Sigma) dissolved in PBS 0.1% BSA for 1 h. Nuclei are directly revealed by 0.1 mg/ml 4',6-Diamidino-2-phenylindole dihydrochloride (DAPI, Sigma),

and the cytoskeleton is visualized by 50 µg/ml phalloïdin-FITC (Sigma), both diluted in PBS 0.1% BSA solution. Samples are then washed in PBS, mounted in Prolon gold® (Invitrogen), and examined using a LSM710 confocal microscope (Carl Zeiss). The experiment was performed two times independently.

Luciferase activity

Cross-linked $(PLL\text{-}PGA)_{14}$ films (non-porous) and cross-linked $([PLL\text{-}PGA]_5\text{-}PLL\text{-}NP)_2\text{-}(PLL\text{-}PGA)_2$ films treated with THF (porous) are built on 10 mm glass slides. The films are exposed to 100 µL containing 0, 10, 50, or 500 ng BMP-2 diluted in 1 mM HCl, for 16 h at 4 °C and rinsed with PBS pH 7.4. C2C12 BRE/Luc cells are seeded (10 000 cells/cm^2) on the films and cultured for 24 h in complete medium. BRE-Luc cells are murine C2C12 myoblasts modified with a luciferase gene fused to a BMP-responsive element (BRE).[28]

Luciferase activity is determined via the quantification of luciferase expression using Bright-Glo™ Luciferase Assay System (Promega). The luminescence signal is measured after 10 min via a luminometer (Sirius Berthold Detection systems), and is proportional to luciferase expression. The measured luciferase activity is directly related to extent of interaction with active BMP-2.

C2C12 differentiation

C2C12 cells (10 000 cells/cm^2) are seeded on Cross-linked $(PLL\text{-}PGA)_{14}$ films (non-porous) and cross-linked $([PLL\text{-}PGA]_5\text{-}PLL\text{-}NP)_2\text{-}(PLL\text{-}PGA)_2$ films treated with THF (porous) loaded or not with 500 ng of BMP-2 (as described above) and cultured for 7 d in DMEM high glucose/Glutamax (Invitrogen) supplemented with 2% horse serum (Invitrogen), 100 U/mL penicillin G and 100 µg/mL streptomycin (Eurobio).

Cell differentiation is investigated following the expression of a late myoblastic marker (myosin heavy chain) and of an early osteoblastic marker (osteopontin) using specific antibodies (Millipore). The immunostaining is performed following the protocol described in the Cell proliferation and morphology section. Succinctly, cells are labeled with mouse anti-myosin heavy chain (MHC, 1:1000), and rabbit anti-osteopontin (1:500), (both from Millipore). Primary antibodies are revealed using Alexa Fluor 488 or Alexa Fluor 633-conjugated goat anti-mouse or anti-rabbit antibodies (1:400, Invitrogen) as secondary antibodies. Samples are examined using a LSM710 confocal microscope (Carl Zeiss).

Statistical analysis

Data are analyzed using Instat statistical software (GraphPad Software). Statistical significance between groups is assessed by one-way analysis of variance (ANOVA) followed by Student–Newman–Keuls multiple comparison tests for cell proliferation.

Experimental results are expressed as means ± standard deviation. Statistical significance is taken for values of $P < 0.05$.

Disclosure of Potential Conflicts of Interest

No potential conflicts of interest were disclosed.

Acknowledgments

The authors graciously acknowledge Delphine Logeart-Avramouglou (Laboratory of Bioengineering and Biomechanics for Bone and Articulations, UMR 7052, CNRS, University Paris Diderot) for the kind gift of C2C12 and C2C12 BRE/Luc cells, Guy Ladam (Laboratoire de Biophysique et Biomatériaux (La2B), SMS EA 3233, IMR FED 4114, Université de Rouen, Centre Universitaire d'Evreux) for assistance with QCM-D measurements, CSM Instruments SA for assistance in nanoindentation experiments, and the US National Science Foundation for financial support through CBET-0756323 and CBET-1066994.

Supplemental Materials

Supplemental materials may be found here:
www.landesbioscience.com/journals/biomatter/article/28823

References

1. Decher G. Fuzzy Nanoassemblies: Toward Layered Polymeric Multicomposites. Science 1997; 277:1232-7; http://dx.doi.org/10.1126/science.277.5330.1232
2. Tang Z, Wang Y, Podsiadlo P, Kotov NA. Biomedical Applications of Layer-by-Layer Assembly: From Biomimetics to Tissue Engineering. Adv Mater 2006; 18:3203-24; http://dx.doi.org/10.1002/adma.200600113
3. Picart C. Polyelectrolyte multilayer films: from physico-chemical properties to the control of cellular processes. Curr Med Chem 2008; 15:685-97; PMID:18336282; http://dx.doi.org/10.2174/092986708783885219
4. Boudou T, Crouzier T, Ren K, Blin G, Picart C. Multiple functionalities of polyelectrolyte multilayer films: new biomedical applications. Adv Mater 2010; 22:441-67; PMID:20217734; http://dx.doi.org/10.1002/adma.200901327
5. Gribova V, Auzely-Velty R, Picart C. Polyelectrolyte Multilayer Assemblies on Materials Surfaces: From Cell Adhesion to Tissue Engineering. Chem Mater 2011; 24:854-69; http://dx.doi.org/10.1021/cm2032459
6. Jessel N, Atalar F, Lavalle P, Mutterer J, Decher G, Schaaf P, et al. Bioactive Coatings Based on a Polyelectrolyte Multilayer Architecture Functionalized by Embedded Proteins. Adv Mater 2003; 15:692-5; http://dx.doi.org/10.1002/adma.200304634
7. Benkirane-Jessel N, Lavalle P, Hübsch E, Holl V, Senger B, Haïkel Y, et al. Short-Time Tuning of the Biological Activity of Functionalized Polyelectrolyte Multilayers. Adv Funct Mater 2005; 15:648-54; http://dx.doi.org/10.1002/adfm.200400129
8. Wood KC, Chuang HF, Batten RD, Lynn DM, Hammond PT. Controlling interlayer diffusion to achieve sustained, multiagent delivery from layer-by-layer thin films. Proc Natl Acad Sci U S A 2006; 103:10207-12; PMID:16801543; http://dx.doi.org/10.1073/pnas.0602884103
9. Macdonald ML, Rodriguez NM, Shah NJ, Hammond PT. Characterization of tunable FGF-2 releasing polyelectrolyte multilayers. Biomacromolecules 2010; 11:2053-9; PMID:20690713; http://dx.doi.org/10.1021/bm100413w
10. Macdonald ML, Samuel RE, Shah NJ, Padera RF, Beben YM, Hammond PT. Tissue integration of growth factor-eluting layer-by-layer polyelectrolyte multilayer coated implants. Biomaterials 2011; 32:1446-53; PMID:21084117; http://dx.doi.org/10.1016/j.biomaterials.2010.10.052
11. Flessner RM, Yu Y, Lynn DM. Rapid release of plasmid DNA from polyelectrolyte multilayers: a weak poly(acid) approach. Chem Commun (Camb) 2011; 47:550-2; PMID:21103586; http://dx.doi.org/10.1039/c0cc02926b
12. Jewell CM, Lynn DM. Multilayered polyelectrolyte assemblies as platforms for the delivery of DNA and other nucleic acid-based therapeutics. Adv Drug Deliv Rev 2008; 60:979-99; PMID:18395291; http://dx.doi.org/10.1016/j.addr.2008.02.010
13. Liu X, Zhang J, Lynn DM. Ultrathin Multilayered Films that Promote the Release of Two DNA Constructs with Separate and Distinct Release Profiles. Adv Mater 2008; 20:4148-53; PMID:19890379
14. Wittmer CR, Phelps JA, Saltzman WM, Van Tassel PR. Fibronectin terminated multilayer films: protein adsorption and cell attachment studies. Biomaterials 2007; 28:851-60; PMID:17056106; http://dx.doi.org/10.1016/j.biomaterials.2006.09.037
15. Wittmer CR, Phelps JA, Lepus CM, Saltzman WM, Harding MJ, Van Tassel PR. Multilayer nanofilms as substrates for hepatocellular applications. Biomaterials 2008; 29:4082-90; PMID:18653230; http://dx.doi.org/10.1016/j.biomaterials.2008.06.027

16. Phelps JA, Morisse S, Hindié M, Degat MC, Pauthe E, Van Tassel PR. Nanofilm biomaterials: localized cross-linking to optimize mechanical rigidity and bioactivity. Langmuir 2011; 27:1123-30; PMID:21182246; http://dx.doi.org/10.1021/la104156c
17. Ren K, Crouzier T, Roy C, Picart C. Polyelectrolyte multilayer films of controlled stiffness modulate myoblast cells differentiation. Adv Funct Mater 2008; 18:1378-89; PMID:18841249; http://dx.doi.org/10.1002/adfm.200701297
18. Schneider A, Francius G, Obeid R, Schwinté P, Hemmerlé J, Frisch B, Schaaf P, Voegel JC, Senger B, Picart C. Polyelectrolyte multilayers with a tunable Young's modulus: influence of film stiffness on cell adhesion. Langmuir 2006; 22:1193-200; PMID:16430283; http://dx.doi.org/10.1021/la0521802
19. Richert L, Boulmedais F, Lavalle P, Mutterer J, Ferreux E, Decher G, Schaaf P, Voegel JC, Picart C. Improvement of stability and cell adhesion properties of polyelectrolyte multilayer films by chemical cross-linking. Biomacromolecules 2004; 5:284-94; PMID:15002986; http://dx.doi.org/10.1021/bm0342281
20. Wu C, Aslan S, Gand A, Wolenski JS, Pauthe E, Van Tassel PR. Porous Nanofilm Biomaterials Via Templated Layer-by-Layer Assembly. Adv Funct Mater 2013; 23:66-74; http://dx.doi.org/10.1002/adfm.201201042
21. Bessa PC, Casal M, Reis RL. Bone morphogenetic proteins in tissue engineering: the road from laboratory to clinic, part II (BMP delivery). J Tissue Eng Regen Med 2008; 2:81-96; PMID:18383454; http://dx.doi.org/10.1002/term.74
22. Carragee EJ, Hurwitz EL, Weiner BK. A critical review of recombinant human bone morphogenetic protein-2 trials in spinal surgery: emerging safety concerns and lessons learned. Spine J 2011; 11:471-91; PMID:21729796; http://dx.doi.org/10.1016/j.spinee.2011.04.023
23. Carragee EJ, Chu G, Rohatgi R, Hurwitz EL, Weiner BK, Yoon ST, Comer G, Kopjar B. Cancer risk after use of recombinant bone morphogenetic protein-2 for spinal arthrodesis. J Bone Joint Surg Am 2013; 95:1537-45; PMID:24005193; http://dx.doi.org/10.2106/JBJS.L.01483
24. Oliver WC, Pharr GM. An improved technique for determining hardness and elastic modulus using load and displacement sensing indentation experiments. J Mat Res 1992; 7:1564-8; http://dx.doi.org/10.1557/JMR.1992.1564
25. Picart C, Mutterer J, Richert L, Luo Y, Prestwich GD, Schaaf P, Voegel JC, Lavalle P. Molecular basis for the explanation of the exponential growth of polyelectrolyte multilayers. Proc Natl Acad Sci U S A 2002; 99:12531-5; PMID:12237412; http://dx.doi.org/10.1073/pnas.202486099
26. Crouzier T, Ren K, Nicolas C, Roy C, Picart C. Layer-by-layer films as a biomimetic reservoir for rhBMP-2 delivery: controlled differentiation of myoblasts to osteoblasts. Small 2009; 5:598-608; PMID:19219837; http://dx.doi.org/10.1002/smll.200800804
27. Ren K, Fourel L, Rouvière CG, Albiges-Rizo C, Picart C. Manipulation of the adhesive behaviour of skeletal muscle cells on soft and stiff polyelectrolyte multilayers. Acta Biomater 2010; 6:4238-48; PMID:20601233; http://dx.doi.org/10.1016/j.actbio.2010.06.014
28. Logeart-Avramoglou D, Bourguignon M, Oudina K, Ten Dijke P, Petite H. An assay for the determination of biologically active bone morphogenetic proteins using cells transfected with an inhibitor of differentiation promoter-luciferase construct. Anal Biochem 2006; 349:78-86; PMID:16307714; http://dx.doi.org/10.1016/j.ab.2005.10.030
29. Katagiri T, Yamaguchi A, Komaki M, Abe E, Takahashi N, Ikeda T, Rosen V, Wozney JM, Fujisawa-Sehara A, Suda T. Bone morphogenetic protein-2 converts the differentiation pathway of C2C12 myoblasts into the osteoblast lineage. J Cell Biol 1994; 127:1755-66; PMID:7798324; http://dx.doi.org/10.1083/jcb.127.6.1755
30. Katagiri T, Akiyama S, Namiki M, Komaki M, Yamaguchi A, Rosen V, Wozney JM, Fujisawa-Sehara A, Suda T. Bone morphogenetic protein-2 inhibits terminal differentiation of myogenic cells by suppressing the transcriptional activity of MyoD and myogenin. Exp Cell Res 1997; 230:342-51; PMID:9024793; http://dx.doi.org/10.1006/excr.1996.3432
31. Discher DE, Janmey P, Wang YL. Tissue cells feel and respond to the stiffness of their substrate. Science 2005; 310:1139-43; PMID:16293750; http://dx.doi.org/10.1126/science.1116995
32. Thompson MT, Berg MC, Tobias IS, Rubner MF, Van Vliet KJ. Tuning compliance of nanoscale polyelectrolyte multilayers to modulate cell adhesion. Biomaterials 2005; 26:6836-45; PMID:15972236; http://dx.doi.org/10.1016/j.biomaterials.2005.05.003
33. Boudou T, Crouzier T, Nicolas C, Ren K, Picart C. Polyelectrolyte multilayer nanofilms used as thin materials for cell mechano-sensitivity studies. Macromol Biosci 2011; 11:77-89; PMID:21038350; http://dx.doi.org/10.1002/mabi.201000301
34. Shah NJ, Hong J, Hyder MN, Hammond PT. Osteophilic multilayer coatings for accelerated bone tissue growth. Adv Mater 2012; 24:1445-50; PMID:22311551; http://dx.doi.org/10.1002/adma.201104475
35. Shah NJ, Hyder MN, Moskowitz JS, Quadir MA, Morton SW, Seeherman HJ, Padera RF, Spector M, Hammond PT. Surface-mediated bone tissue morphogenesis from tunable nanolayered implant coatings. Sci Transl Med 2013; 5:91ra83; PMID:23803705; http://dx.doi.org/10.1126/scitranslmed.3005576
36. Bechler SL, Si Y, Yu Y, Ren J, Liu B, Lynn DM. Reduction of intimal hyperplasia in injured rat arteries promoted by catheter balloons coated with polyelectrolyte multilayers that contain plasmid DNA encoding PKCδ. Biomaterials 2013; 34:226-36; PMID:23069712; http://dx.doi.org/10.1016/j.biomaterials.2012.09.010
37. Saurer EM, Jewell CM, Roenneburg DA, Bechler SL, Torrealba JR, Hacker TA, Lynn DM. Polyelectrolyte multilayers promote stent-mediated delivery of DNA to vascular tissue. Biomacromolecules 2013; 14:1696-704; PMID:23597075; http://dx.doi.org/10.1021/bm4005222
38. Schneider A, Richert L, Francius G, Voegel JC, Picart C. Elasticity, biodegradability and cell adhesive properties of chitosan/hyaluronan multilayer films. Biomed Mater 2007; 2:S45-51; PMID:18458419; http://dx.doi.org/10.1088/1748-6041/2/1/S07
39. Schneider A, Vodouhê C, Richert L, Francius G, Le Guen E, Schaaf P, Voegel JC, Frisch B, Picart C. Multifunctional polyelectrolyte multilayer films: combining mechanical resistance, biodegradability, and bioactivity. Biomacromolecules 2007; 8:139-45; PMID:17206799; http://dx.doi.org/10.1021/bm060765k
40. Etienne O, Schneider A, Taddei C, Richert L, Schaaf P, Voegel JC, Egles C, Picart C. Degradability of polysaccharides multilayer films in the oral environment: an in vitro and in vivo study. Biomacromolecules 2005; 6:726-33; PMID:15762636; http://dx.doi.org/10.1021/bm049425u
41. Picart C, Schneider A, Etienne O, Mutterer J, Schaaf P, Egles C, et al. Controlled degradability of polysaccharide multilayer films in vitro and in vivo. Adv Funct Mater 2005; 15:1771-80; http://dx.doi.org/10.1002/adfm.200400588
42. Vodouhê C, Le Guen E, Garza JM, Francius G, Déjugnat C, Ogier J, Schaaf P, Voegel JC, Lavalle P. Control of drug accessibility on functional polyelectrolyte multilayer films. Biomaterials 2006; 27:4149-56; PMID:16600366; http://dx.doi.org/10.1016/j.biomaterials.2006.03.024
43. Crouzier T, Szarpak A, Boudou T, Auzély-Velty R, Picart C. Polysaccharide-blend multilayers containing hyaluronan and heparin as a delivery system for rhBMP-2. Small 2010; 6:651-62; PMID:20155753; http://dx.doi.org/10.1002/smll.200901728
44. Crouzier T, Fourel L, Boudou T, Albigès-Rizo C, Picart C. Presentation of BMP-2 from a soft biopolymeric film unveils its activity on cell adhesion and migration. Adv Mater 2011; 23:H111-8; PMID:21433098; http://dx.doi.org/10.1002/adma.201004637
45. Crouzier T, Sailhan F, Becquart P, Guillot R, Logeart-Avramoglou D, Picart C. The performance of BMP-2 loaded TCP/HAP porous ceramics with a polyelectrolyte multilayer film coating. Biomaterials 2011; 32:7543-54; PMID:21783243; http://dx.doi.org/10.1016/j.biomaterials.2011.06.062
46. Voinova M, Rodahl M, Jonson M, Kasemo B. Viscoelastic acoustic response of layered polymer films at fluid-solid interfaces: continuum mechanics approach. Phys Scr 1999; 59:391-6; http://dx.doi.org/10.1238/Physica.Regular.059a00391